

# Solution, solid phase and computational structures of apicidin and its backbone-reduced analogs

MICHAEL KRANZ,<sup>a\*</sup> PETER JOHN MURRAY,<sup>a</sup> STEPHEN TAYLOR,<sup>a</sup> RICHARD J. UPTON,<sup>b</sup> WILLIAM CLEGG<sup>c</sup> and MARK R. J. ELSEGOOD<sup>c</sup>

<sup>a</sup> GlaxoSmithKline Cambridge Chemistry Laboratory, Department of Chemistry, University of Cambridge, Cambridge, CB2 1EW, UK

<sup>b</sup> Physical Sciences, GlaxoSmithKline, Medicines Research Centre, Stevenage SG1 2NY, UK

<sup>c</sup> School of Natural Sciences (Chemistry), University of Newcastle, Newcastle upon Tyne, NE1 7RU, UK

Received 24 July 2005; Revised 25 August 2005; Accepted 10 October 2005

**Abstract:** The recently isolated broad-spectrum antiparasitic apicidin (**1**) is one of the few naturally occurring cyclic tetrapeptides (CTP). Depending on the solvent, the backbone of **1** exhibits two  $\gamma$ -turns (in  $\text{CH}_2\text{Cl}_2$ ) or a  $\beta$ -turn (in DMSO), differing solely in the rotation of the plane of one of the amide bonds. In the X-ray crystal structure, the peptidic C=Os and NHs are on opposite sides of the backbone plane, giving rise to infinite stacks of cyclotetrapeptides connected by three intermolecular hydrogen bonds between the backbones. Conformational searches (Amber force field) on a truncated model system of **1** confirm all three backbone conformations to be low-energy states. The previously synthesized analogs of **1** containing a reduced amide bond exhibit the same backbone conformation as **1** in DMSO, which is confirmed further by the X-ray crystal structure of a model system of the desoxy analogs of **1**. This similarity helps in explaining why the desoxy analogs retain some of the antiprotozoal activities of apicidin. The backbone-reduction approach designed to facilitate the cyclization step of the acyclic precursors of the CTPs seems to retain the conformational preferences of the parent peptide backbone. Copyright © 2005 European Peptide Society and John Wiley & Sons, Ltd.

**Keywords:** cyclic tetrapeptide; cyclization; peptide synthesis; conformational analysis; peptide NMR; peptide X ray

## INTRODUCTION

A small group of cyclic tetrapeptide (CTP) natural products (Figure 1) interfere with the regulatory process in the control of chromatin structure and gene expression via a pharmaceutically yet unexploited mechanism by interacting with a nuclear enzyme, histone deacetylase [1,2]. The potent broad-spectrum antiparasitic agent apicidin (**1**) has been shown to have activity against malaria parasites *Plasmodium falciparum* *in vitro* and *Plasmodium berghei* in mice [3,4]. Apicidin was originally isolated from cultures of *Fusarium pallidoroseum* [3] and several syntheses have subsequently been published [5,6].

However, the generation of SAR data for apicidin derivatives had to rely on degradation experiments rather than the more convenient forward synthesis [7,8]. The reason is the difficulty in achieving the intramolecular cyclization of the linear tetrapeptide precursor due to intermolecular competition reactions [9–12]. In addition, the differentiation between the CTP and its dimer, cyclo-octapeptide (COP), can be equivocal [7]. As an alternative approach to the 12-membered ring template, we had chosen to synthesize a backbone-reduced analog [13]. As the cyclization step of the

linear tetrapeptide is the synthetically most challenging obstacle, we have calculated the transition state energies (semiempirical AM1 method) of the possible amide bond formations in some monodesoxy model compounds. The energetically most favoured cyclization reaction to build the prospective 12-membered ring is predicted for the secondary D-amino acid at the C-terminus and the reduced amide bond in the central position of the linear precursor (Scheme 1) [13]. In a model system for apicidin, the monodesoxy amide linear precursor has given the cyclic tetrapeptoid **2** in high yield (82%). Several monodesoxy compounds, more closely related to apicidin, have also been synthesized (**3–5**) and were shown to retain some of its biological activities [13].

We present herein a detailed analysis of the solid phase and solution structures of apicidin and

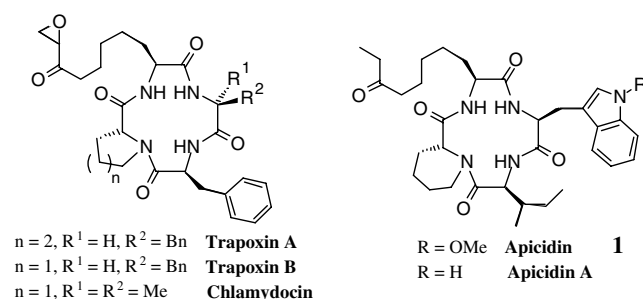
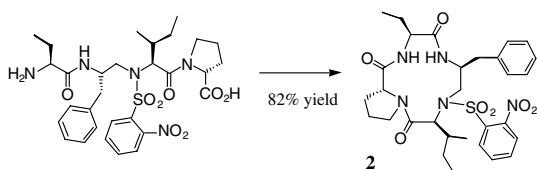


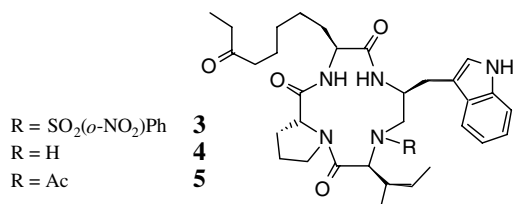
**Figure 1** Naturally occurring CTPs.

\*Correspondence to: M. Kranz, GlaxoSmithKline, Medicines Research Centre, Gunnelswood Road, Stevenage SG1 2NY, UK; e-mail: michael.j.kranz@gsk.com



**Scheme 1** Synthesis of a backbone-reduced truncated apicidin analog.

several desoxy analogs supported by computational data.



## METHODS

NMR spectra were recorded on a Varian Inova 750 MHz at 25 °C. Signals are referenced to the residual DMSO signal at 2.5 ppm unless otherwise stated. <sup>1</sup>H NMR resonance assignments are based on the two-dimensional <sup>1</sup>H-<sup>1</sup>H COSY, <sup>1</sup>H-<sup>13</sup>C HMQC and phase-sensitive rotating frame NOE (ROESY, 250-ms mixing time, 3-kHz spin lock) spectra obtained with the standard Varian pulse sequences. Analytical HPLC was run on a Hewlett-Packard 1050 instrument using an ABZ + Plus Supelcosil column (33 mm, 4.6 mm, 3 μm) with 7 min gradient time (1 ml/min) 10–95% solvent B in A, then 95% solvent B for 1 min; solvent A: 0.1% TFA in water; solvent B: 0.05% TFA in MeCN/H<sub>2</sub>O (95 : 5); UV detection at 215 nm.

## X-ray crystallography

Data for **1** and **2** were measured on Bruker SMART CCD diffractometers. For **1**, synchrotron radiation ( $\lambda = 0.6875 \text{ \AA}$ ) was used at Daresbury Laboratory SRS. For **2**, Mo K $\alpha$  radiation ( $\lambda = 0.71073 \text{ \AA}$ ) was used.

**Crystal data for 1·0.25CHCl<sub>3</sub>.** C<sub>34</sub>H<sub>47</sub>N<sub>5</sub>O<sub>6</sub>·0.25CHCl<sub>3</sub>,  $M = 651.6$ , crystal dimensions  $0.18 \times 0.06 \times 0.02 \text{ mm}$ , orthorhombic,  $P2_12_12_1$ ,  $a = 19.176(2)$ ,  $b = 20.272(2)$ ,  $c = 38.540(4) \text{ \AA}$ ,  $V = 14982(3) \text{ \AA}^3$ ,  $Z = 16$ ,  $\rho_{\text{calcd}} = 1.156 \text{ g/cm}^3$ ; 78 700 reflections measured, 21 428 independent,  $R = 0.097$  ( $F$  values, 11 662 reflections with  $F_o^2 > 2\sigma(F_o^2)$ ),  $R_w = 0.263$  ( $F^2$  values, all data),  $S = 0.962$ , 1652 parameters, 1110 restraints, residual electron density  $0.56/-0.30 \text{ e/\AA}^3$ .

**Crystal data for 2.** C<sub>30</sub>H<sub>39</sub>N<sub>5</sub>O<sub>7</sub>S,  $M = 613.7$ , crystal dimensions  $0.57 \times 0.42 \times 0.10 \text{ mm}$ , orthorhombic,  $P2_12_12_1$ ,  $a = 10.1858(5)$ ,  $b = 15.9243(8)$ ,  $c = 18.8691(10) \text{ \AA}$ ,  $V = 3060.6(3) \text{ \AA}^3$ ,  $Z = 4$ ,  $\rho_{\text{calcd}} = 1.332 \text{ g/cm}^3$ ; 19 866 reflections measured, 7348 independent,  $R = 0.044$  ( $F$  values, 6131 reflections with  $F_o^2 > 2\sigma(F_o^2)$ ),  $R_w = 0.103$  ( $F^2$  values, all data),  $S = 0.990$ , 392 parameters, no restraints, residual electron density  $0.69/-0.62 \text{ e/\AA}^3$ .

The crystallographic results have been deposited at the Cambridge Crystallographic Data Centre. For **1**, the deposition number is CCDC 274844; for **2**, a preliminary report of which was published previously [13], the REFCODE is QIRRU.

## Calculations

Calculations were carried out on a Silicon Graphics Indigo 2 with MacroModel (version 5.5) using the BatchMin facility [14]. Conformational searches used the standard settings of the Monte-Carlo multiple minimum search method [15] and the conjugate gradient method for energy minimizations employing the Amber force field [16,17] (implicit hydrogens) and the MacroModel-internal GB/SA solvation treatment for water [18]. No conformational constraints were imposed and the default torsional constraint on the amide bonds was removed during the searches.

## RESULTS AND DISCUSSION

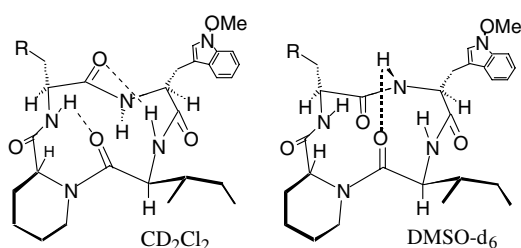
### Apicidin

In the original structural analysis of apicidin, undisclosed NOE data (in CD<sub>2</sub>Cl<sub>2</sub> and C<sub>5</sub>H<sub>5</sub>N) as well as the temperature and concentration dependence of NH chemical shifts were given as evidence for three intramolecular H-bonds, leading to a set of three 7-membered rings within the apicidin backbone [3]. However, we could not accommodate simultaneously more than two of these  $\gamma$ -turns within this CTP, neither in a ball-and-stick model nor in computer simulations (*vide infra*). Our proton chemical shifts in CD<sub>2</sub>Cl<sub>2</sub> agree without exception with those published (CD<sub>2</sub>Cl<sub>2</sub>) [3], but the trends of our amide protons' temperature dependences (CD<sub>2</sub>Cl<sub>2</sub>) are distinct from the ones in pyridine, published recently by the same group (Table 1) [19]. Whereas the relatively large values in pyridine (−4 to −9 ppb/°C) [19] seem to indicate solvent exposure of all 3 amide protons [20], much smaller values in CD<sub>2</sub>Cl<sub>2</sub> for 2 amide protons (0 to −2 ppb/°C) give rise to the backbone geometry depicted in Figure 2:  $\gamma$ -turns at Trp(OMe) and *D*-pipercolic acid (*D*-Pip), while the Trp(OMe) amide proton is solvent-exposed (−6 ppb/°C). All our other NMR data (couplings, ROEs) support the CD<sub>2</sub>Cl<sub>2</sub> backbone configuration shown in Figure 2. The third H-bond has previously been postulated between the Trp(OMe) NH and Pip C=O [3,19]; however, this cannot be realized in the model in Figure 2. This H-bond is 3.4 Å long in our computed structure (Figure 4; 2.2–4 Å in the MD simulations of Ref. 19).

In DMSO solution, the NMR spectra indicate that three conformations are present at room temperature (ratio of ca 13 : 3.5 : 1). The three different forms exhibit show exchange of magnetisation on the NMR time scale. In the major form, all peptide bonds are again in the *trans* configuration, but now all three NHs are *anti* with respect to their intra-residue  $\alpha$  protons, as indicated by

**Table 1** Selected NMR data of Apicidin in CD<sub>2</sub>Cl<sub>2</sub> and DMSO-d<sub>6</sub> at 750 MHz and in C<sub>5</sub>H<sub>5</sub>N at 400/500 MHz<sup>a</sup>

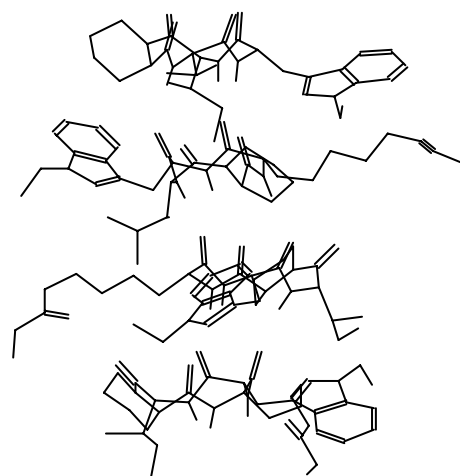
Residue	Solvent	Strong ROE $\alpha$ CH/NH	$^3J$ $\alpha$ CHNH [Hz]	$\delta\Delta/T$ NH [ppb/K]
Aoda	CD <sub>2</sub> Cl <sub>2</sub>	No	10.5	0.0 <sup>b</sup>
	DMSO-d <sub>6</sub>	No	10.5	+0.8 <sup>b</sup>
	C <sub>5</sub> D <sub>5</sub> N <sup>a</sup>	—	—	-5.1 <sup>c</sup>
Trp(OMe)	CD <sub>2</sub> Cl <sub>2</sub>	Yes	7.0	-6.0 <sup>b</sup>
	DMSO-d <sub>6</sub>	No	9.5	+0.8 <sup>b</sup>
	C <sub>5</sub> D <sub>5</sub> N <sup>a</sup>	—	—	-9.3 <sup>c</sup>
Ile	CD <sub>2</sub> Cl <sub>2</sub>	No	10.5	-2.0 <sup>b</sup>
	DMSO-d <sub>6</sub>	No	10.0	-3.7 <sup>b</sup>
	C <sub>5</sub> D <sub>5</sub> N <sup>a</sup>	—	—	-4.0 <sup>c</sup>

<sup>a</sup> Ref 19.<sup>b</sup>  $\Delta T = 25-65^\circ\text{C}$ .<sup>c</sup>  $\Delta T = -10-70^\circ\text{C}$ .**Figure 2** Backbone conformations of apicidine in CD<sub>2</sub>Cl<sub>2</sub> and DMSO solution as deduced from NMR data (R = heptan-5-one as part of Aoda).

the large intra-residue coupling constants and relatively small ROEs (Table 1). Hence, the rotation of the amide bond between (2*S*)-2-amino-8-oxodecanoic acid (Aoda) and TrpOMe by *ca* 180° with regard to the backbone conformation in CD<sub>2</sub>Cl<sub>2</sub> allows the NH of TrpOMe to form an H-bond with the carbonyl of Ile, consistent with the small temperature dependence of the NH chemical shift observed (Figure 2; Table 1). This arrangement approximates a  $\beta$ -turn with *D*-Pip and Aoda in the *i* + 1 and *i* + 2 positions respectively.

**Crystallography.** Thin needles of apicidin were grown in a chloroform/methanol solution by vapour diffusion of pentane. Owing to their small size, synchrotron radiation had to be used for the X-ray analysis. The data obtained yielded no solution with conventional methods of structure solution. The structure could, however, be solved with the new SHELXD program [21,22].

The asymmetric unit is composed of four molecules of apicidin that are structurally distinct only in the orientation of their side chains; the backbone remains essentially the same (Figure 3), together with a disordered molecule of chloroform. The molecules form an infinite array hydrogen-bonded through the amidic carbonyls of one molecule to the amide protons of the next. This arrangement with all four carbonyl groups on the same side of the backbone plane bears no

**Figure 3** The four molecules of apicidin in the asymmetric unit of the X-ray crystal structure.

resemblance to any of the solution structures (Figure 2). However, this conformation could be one of the minor forms seen in the DMSO solution. The amide bond between Ile and Pip is in the *cis* configuration.

This columnar stacking of cyclic peptides has been targeted by several groups trying to create nanotubes as artificial transmembrane ion channels [23–25]. A CTP with alternating  $\alpha$ - and  $\beta$ -amino acids [26], cyclic octamers with alternating *L*- and *D*- $\alpha$ -amino acids [27] or a CTP comprising exclusively  $\beta$ -amino acids [25] allow for a flat arrangement of the peptide backbone with the planes of the amidic linkages perpendicular to it. However, only the  $\beta$ -amino acid CTPs exhibit the carbonyl groups and NH on opposite sides of the backbone, [25] giving rise to considerable channel K<sup>+</sup> conductance [28].

**Computation.** The conformational space can be explored in a more systematic fashion by computational methods. The Amber force field within MacroModel was

employed to reminimize a single aggregate of four apicidin molecules taken from the asymmetric unit of the X-ray crystal structure. In this supermolecule as well as in calculations for each individual molecule, only minor adjustments of the backbone or the side chains occur, thus vindicating the suitability of the Amber force field for these constrained CTPs. The conformational preferences of the CTP backbone were assessed by a Monte Carlo conformational search of the truncated apicidin analog c[Ala-Ala-Ala-*D*-Pip] (**6**) retaining the crucial stereochemistries and the *N*-substitution.

The lowest energy structure exhibits the same features as the DMSO solution structure: with four *trans* amide bonds and all intra-residue  $\alpha$ CH-NH *anti* (Figure 4). The close proximity of the three NHs in the computational model (2.2–3.5 Å) is corroborated by the medium-to-strong ROEs in the NMR spectra. The second lowest energy conformation of **6** (+6.4 kJ/mol) contains a *cis*-arrangement at the tertiary amide, aligning all four carbonyls on the same side of the backbone plane. The overlay of this structure with the backbone of the X-ray crystal structure shows hardly any deviation. As mentioned before, this backbone conformation could be present as one of the minor components in DMSO solution. The peptide bond arrangement seen in CD<sub>2</sub>Cl<sub>2</sub> solution is found in the fourth lowest energy structure (+11.8 kJ/mol; Figure 4): two H-bonds (1.9, 2.5 Å) are part of 2 $\gamma$ -turns; the third H-bond proposed by the Merck group is 3.4 Å long in this model. The third lowest energy conformation (+109 kJ/mol) is similar to the second lowest one.

The different conformations in solution and the crystal can be rationalized on the basis of the calculated

dipole moments. The lowest energy structure (Figure 4) has three carbonyls on the same side of the backbone plane (7.2 Debye), whereas it is four carbonyls for the second lowest (9.0 Debye) and two on either side for the fourth lowest energy structure (0.0 Debye). Just as the more polar solvent (DMSO) favours a ring conformation exhibiting a higher dipole moment (7.2 Debye) than does the less polar CD<sub>2</sub>Cl<sub>2</sub> (0.0 Debye), it could be argued that the highest dipole moment of the low-energy conformations (9.0 Debye) might lead to faster crystal growth (at least in one direction), and this dipole moment will be further augmented by the intermolecular hydrogen bonding.

### Desoxy-apicidin

The concept of reducing a backbone amide carbonyl to facilitate tetrapeptide cyclization has been successfully tested on a truncated apicidin analog (Scheme 1) [13]. The influence of the backbone modifications can be probed by computational studies on model systems. Introducing proline for pipecolic acid in **6** (**7**) does not change the geometries of the lowest energy structures (Figure 4 and 5), but only renders the *cis* arrangement less favourable (+16.7 kJ/mol). Backbone reduction, as shown in Figure 5 (**8**), does not change the conformational preferences in this model system.

According to the NMR spectra of **2–5** in DMSO, the amide bonds are predominantly in the *trans* configuration and all of the intra-residue  $\alpha$ CH/NH bonds are *anti* (Table 2). More significantly, the small temperature dependence of the NH chemical shifts of the aromatic residues could be due to the same  $\beta$ -turn observed for apicidin in DMSO solution (Figure 2).

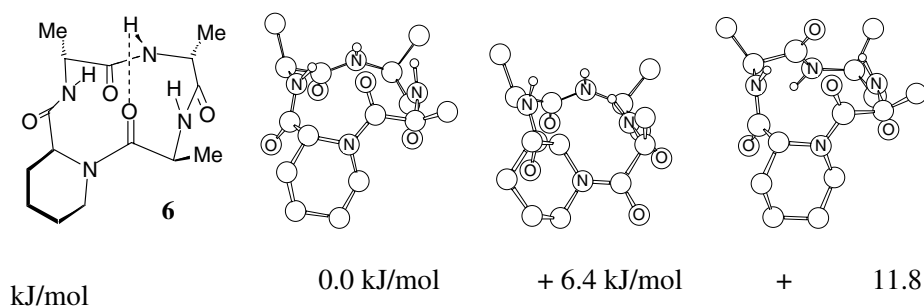


**Figure 4** Computational model of apicidin (c[Ala-Ala-Ala-*D*-Pip]; **6**) and the lowest, second and fourth lowest energy structures (Amber force field).

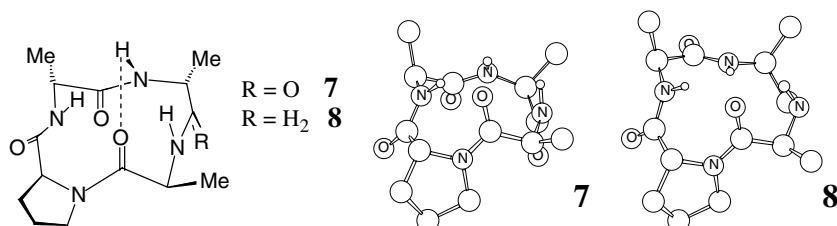


**Figure 5** Lowest energy structures of the *D*-Pro (**7**) and backbone-reduced *D*-Pro analogs (**8**) of apicidin.

**Table 2** Selected NMR Data of **2–5** in DMSO- $d_6$  at 750 MHz

Compound	Residue	Strong ROE $\alpha$ CH/NH	$^3J$ $\alpha$ -CHNH [Hz]	$\delta\Delta/T$ NH [ppb/K] <sup>c</sup>
2	Abu	No	8.0	7
	m-Phe <sup>a</sup>	No	6.5	0
3	Aoda	No	8.0	6.5
	m-Trp <sup>b</sup>	No	6.5	0.4
4	Aoda	No	7.0	7.7
	m-Trp <sup>b</sup>	No	8.0	1.3
5	Aoda	No	7.0	7
	m-Trp <sup>b</sup>	No	6.0	0.2

<sup>a</sup> m-Phe = desoxy-Phe.

<sup>b</sup> m-Trp = desoxy-Trp.

<sup>c</sup>  $\Delta T = 25\text{--}65^\circ\text{C}$ .



**Figure 6** Two views of the molecular structure of the desoxy-apicidin analog **2** in the crystal (the intramolecular hydrogen bond is drawn as a dotted line).

The bulky nitrophenyl substituent in **2** and **5** has surprisingly little influence on the backbone orientation according to the NMR data. A medium-sized ROE coupling between the *ortho* hydrogen of the nitrophenyl group and one of the  $\delta$ -protons of *D*-Pro suggests this aryl to be close to the peptide backbone. The presence of a single set of signals for each of the four compounds shows that the modified peptide backbone does not allow for a significant degree of flexibility (for compound **5**, a minor component is due to a rotation of the acetyl group).

The truncated desoxy-apicidin analog **2** was crystallized from dichloromethane by vapour diffusion of pentane and the molecular structure is shown in Figure 6 [13]. The nitrophenyl group is located perpendicular to and just underneath the peptide backbone, as found in solution. All three amide bonds are *trans* and the reduced amide bond is in a pseudo-*trans* arrangement. An intramolecular hydrogen bond (2.08 Å) between the NH of the desoxy-Phe and the carbonyl of Ile is part of the  $\beta$ -turn with *D*-Pro and Abu at the  $i+1$  and  $i+2$  positions. This backbone conformation is in agreement with those derived from the NMR data in DMSO solution of apicidin (**1**) and its desoxy derivatives **2–5**.

## CONCLUSIONS

The previously reported solution structure ( $\text{CD}_2\text{Cl}_2$ ) of the CTP apicidin exhibits two  $\gamma$ -turns within the 12-membered ring backbone. In DMSO, one amide bond has changed its orientation relative to the backbone plane, giving rise to a single backbone hydrogen bond forming part of a  $\beta$ -turn. This arrangement also constitutes the lowest energy structure of a conformational search for a truncated model system. Yet another backbone conformation, which is also low on the computational potential energy surface, is found in the X-ray crystal structure and can be rationalized by the size of the dipole moments. The infinite stacks of hydrogen-bonded peptide backbones with all amidic carbonyl groups pointing in the same direction have previously only been achieved in CTPs made from  $\beta$ -amino acids.

Several desoxy analogs of apicidin assume the same backbone conformation in DMSO as the parent compound. This  $\beta$ -turn geometry is confirmed by the X-ray crystal structure of a slightly truncated desoxy analog of apicidin. These results have two implications: (i) they justify the backbone reduction as a valid approach to new derivatives of apicidin with the potential for similar biological activities [13] and (ii) they also give credence to the predictive power of the Amber force field for these rather constrained small ring systems.

## Acknowledgements

This work was supported by GlaxoSmithKline with an Industrial Trainee Placement (ST), by EPSRC with an equipment grant (WC), and by CCLRC with the award of synchrotron beamtime. We are grateful to Professor George Sheldrick (Göttingen) for his help in structure solution, using a pre-release version of SHELXD.

## Supplementary material available

NMR characterization of **1–4** and the MacroModel output files of **6–8** are available from the authors upon request.

## REFERENCES

- Hassig CA, Schreiber SL. Nuclear histone acetylases and deacetylases and transcriptional regulation: HATs off to HDACs. *Curr. Opin. Chem. Biol.* 1997; **1**: 300–308.
- Pazin MJ, Kadonaga JT. What's up and down with histone deacetylation and transcription? *Cell* 1997; **89**: 325–328.
- Singh SB, Zink DL, Polishook JD, Dombrowski AW, Darkin-Ratray SJ, Schmatz DM, Goetz MA. Apicidins: novel cyclotetrapeptides as coccidiostats and antimalarial agents from *Fusarium pallidroseum*. *Tetrahedron Lett.* 1996; **37**: 8077–8880.
- Darkin-Ratray SJ, Gurnett AM, Myers RW, Dulski PM, Crumley TM, Allocco JJ, Cannova C, Meinke PT, Colletti SL, Bednarek MA, Singh SB, Goetz MA, Dombrowski AW, Polishook JD, Schmatz DM. Apicidin: a novel antiprotozoal agent that inhibits parasite histone deacetylase. *Proc. Natl. Acad. Sci. U.S.A.* 1996; **93**: 13 143–13 147.
- Kuriyama W, Kitahara T. Synthesis of apicidin. *Heterocycles* 2001; **55**: 1–4.
- Mou L, Singh G. Synthesis of (S)-2-amino-8-oxodecanoic acid (Aoda) and apicidin A. *Tetrahedron Lett.* 2001; **42**: 6603–6606.
- Colletti SL, Myers RW, Darkin-Ratray SJ, Gurnett AM, Dulski PM, Galuska S, Allocco JJ, Ayer MB, Li C, Lim J, Crumley TM, Cannova C, Schmatz DM, Wyvratt MJ, Fisher MH, Meinke PT. Broad spectrum antiprotozoal agents that inhibit histone deacetylase: structure-activity relationships of apicidin. Part 1. *Bioorg. Med. Chem. Lett.* 2001; **11**: 107–111.
- Colletti SL, Myers RW, Darkin-Ratray SJ, Gurnett AM, Dulski PM, Galuska S, Allocco JJ, Ayer MB, Li C, Lim J, Crumley TM, Cannova C, Schmatz DM, Wyvratt MJ, Fisher MH, Meinke PT. Broad spectrum antiprotozoal agents that inhibit histone deacetylase: structure-activity relationships of apicidin. Part 2. *Bioorg. Med. Chem. Lett.* 2001; **11**: 113–117, and literature cited therein.
- Schmidt U, Langner J. Cyclotetrapeptides and cyclopentapeptides: occurrence and synthesis. *J. Pept. Res.* 1997; **49**: 67–73.
- Taunton J, Collins JL, Schreiber SL. Synthesis of natural and modified Trapoxins, useful reagents for exploring histone deacetylase function. *J. Am. Chem. Soc.* 1996; **118**: 10 412–14 022.
- Nishino N, Hayashida J, Arai T, Mihara H, Ueno Y, Kumagai H. Cyclo(-arginyl-sarcosyl-aspartyl-phenylglycyl-) 2. Simple synthesis of an RGD-related peptide with inhibitory activity for platelet aggregation. *J. Chem. Soc., Perkin Trans. 1* 1996; 939–946.
- Cavelier-Frontin F, Pèpe G, Verducci J, Siri D, Jacquier R. Prediction of the best linear precursor in the synthesis of cyclotetrapeptides by molecular mechanic calculations. *J. Am. Chem. Soc.* 1992; **114**: 8885–8890.
- Murray PJ, Kranz M, Ladlow M, Taylor S, Berst F, Holmes AB, Keavey KN, Jaxa-Chamiec A, Seale PW, Stead P, Upton RJ, Croft SL, Clegg W, Elsegood MR. The synthesis of cyclic tetrapeptid analogues of the antiprotozoal product apicidin. *Bioorg. Med. Chem. Lett.* 2001; **11**: 773–776.
- Mohamadi F, Richards NGJ, Guida WC, Liskamp R, Lipton M, Caufield C, Chang G, Hendrickson T, Still WC. MacroModel – an integrated software system for modeling organic and bioorganic molecules using molecular mechanics. *J. Comput. Chem.* 1990; **11**: 440–467.
- Saunders M, Houk KN, Wu Y-D, Still WC, Lipton M, Chang G, Guida WC. Conformations of cycloheptadecane. A comparison of methods for conformational searching. *J. Am. Chem. Soc.* 1990; **112**: 1419–1427.
- Weiner SJ, Kollman PA, Case DA, Singh UC, Ghio C, Alagona G, Profeta S Jr, Weiner P. A new force field for molecular mechanical simulation of nucleic acids and proteins. *J. Am. Chem. Soc.* 1984; **106**: 765–784.
- Ferguson DM, Kollman PA. Can the Lennard-Jones 6–12 function replace the 10–12 form in molecular mechanics calculations? *J. Comput. Chem.* 1991; **12**: 620–626.
- Still WC, Tempczyk A, Hawley RC, Hendrickson T. Semianalytical treatment of solvation for molecular mechanics and dynamics. *J. Am. Chem. Soc.* 1990; **112**: 6127–6129.
- Singh SB, Zink DL, Liesch JM, Mosley RT, Dombrowski AW, Bills GF, Darkin-Ratray SJ, Schmatz DM, Goetz MA. Structure and chemistry of apicidins, a class of novel cyclic tetrapeptides without a terminal  $\alpha$ -keto epoxide as inhibitors of histone deacetylase with potent antiprotozoal activities. *J. Org. Chem.* 2002; **67**: 815–825.
- Kessler H. Conformation and biological activity of cyclic peptides. *Angew. Chem., Int. Ed. Engl.* 1982; **21**: 512–523.
- Sheldrick GM. In *Direct Methods for Solving Macromolecular Structures*, Fortier S (ed). Kluwer Academic Publishers: Dordrecht, 1998: 401.
- Uson I, Sheldrick GM. Advances in direct methods for protein crystallography. *Curr. Opin. Struct. Biol.* 1999; **9**: 643–648.
- Tomasic L, Lorenzi GP. Some cyclic oligopeptides with S<sub>2n</sub> symmetry. *Helv. Chim. Acta* 1987; **70**: 1012–1016.
- Ghadiri MR, Granja JR, Milligan RA, McRee DE, Khazanovich N. Self-assembling organic nanotubes based on a cyclic peptide architecture. *Nature* 1993; **366**: 324–327.
- Seebach D, Matthews JL, Meden A, Wessels T, Baerlocher C, McCusker LB. Cyclo- $\beta$ -peptides. Structure and tubular stacking of cyclic tetramers of 3-aminobutanoic acid as determined from powder diffraction data. *Helv. Chim. Acta* 1997; **80**: 173–182.
- Karle IL, Handa BK, Hassall CH. Conformation of the cyclic tetrapeptide L-ser(oxygen bonded to tert-butyl)- $\beta$ -Ala-Gly-L- $\beta$ -Asp(oxygen bonded to methyl) containing a 14-membered ring. *Acta Crystallogr.* 1975; **B31**: 555–560.
- Ghadiri MR, Kobayashi K, Granja JR, Chadha RK, McRee DE. The structural and thermodynamic basis for the formation of self-assembled peptide nanotubes. *Angew. Chem., Int. Ed. Engl.* 1995; **34**: 93–95.
- Clark TD, Buehler LK, Ghadiri MR. Self-assembling cyclic  $\beta$ 3-peptide nanotubes as artificial transmembrane ion channels. *J. Am. Chem. Soc.* 1998; **120**: 651–656.